Global Gyrokinetic Simulation of Electron Temperature Gradient Turbulence and Transport in NSTX Plasmas

S. Ethier 1), W. X. Wang 1), F. Poli 2), S.M. Kaye 1), E. Mazzucato 1), B.P. LeBlanc 1), T. S. Hahm 1), G. Rewoldt 1), W.W. Lee 1), W. M. Tang 1)

1) Princeton Plasma Physics Laboratory, P. O. Box 451, Princeton, New Jersey 08543, USA
2) University of Warwick, Coventry, UK

E-mail contact of main author: ethier@pppl.gov

Abstract

Global, nonlinear gyrokinetic simulations of electron temperature gradient (ETG) driven turbulence were carried out with the GTS code using actual experimental parameters of NSTX discharges. Our simulations reveal remarkable new features with regard to nonlinear spectral dynamics in 2D perpendicular wavenumber space. Specifically, there exists direct, strong energy coupling between high-k ETG modes and electron geodesic acoustic modes (e-GAMs with high frequency and poloidal mode number m = 1). At the same time, zonal flows are generated and continuously grow with a fine radial scale. This direct energy coupling may represent a new insight into the underlying mechanism for nonlinear ETG saturation. It also implies that the collisional damping of zonal flows and e-GAMs may have considerable impact on the formation of the steady state spectrum and saturation level. Further, the ETG fluctuation spectra are characterized by strong anisotropy with $k_r \ll k_\theta$. The $k_\perp$ spectrum of density fluctuations is in general agreement with the experimental measurement using coherent scattering of electromagnetic waves. Within experimental uncertainties in plasma profiles, ETG turbulence is shown to drive experimentally relevant transport for electron heat in NSTX.

1. Introduction

Plasmas in various magnetic fusion experiments universally exhibit anomalous electron energy transport whose origin, however, remains unknown under most circumstances. In the search of one or more candidates for driving this electron transport, short scale fluctuations driven by electron temperature gradient (ETG) modes have been a subject of high interest to experiment [1, 2, 3, 4] simulation and theory. The role of ETG turbulence is an important issue for ITER, for which energy losses are expected to be dominated by electron transport. Using the GTS particle-in-cell (PIC) code [5], global, nonlinear simulations of ETG turbulence for experimental discharges have been carried out with emphasis on direct validation against high-k scattering measurements of electron gyroradius scale fluctuations in NSTX, and quantitatively testing the role of ETG for driving anomalous electron energy transport in experiments. This unique simulation study offers interesting new insight into the characteristics of ETG turbulence under experimental conditions, and into the underlying nonlinear spectral dynamics. The key results of our simulations also include the prediction of significant ETG-induced contributions to anomalous electron heat transport in NSTX, and predicted frequency and wavenumber spectra that are in general agreement with experimental observations.

2. Description of model and simulations

The global kinetic simulation of electron scale turbulence in a real fusion device is truly a grand challenge. Most of the previous theoretical studies of ETG using advanced gyrokinetic codes

were carried out with flux-tube codes in the local approximation and were already very demanding computationally [6, 7, 8]. A few global simulations were also carried out but for very small systems (a$\approx 450\rho_e$) in the idealized large aspect ratio approximation [9, 10]. In this work, the GTS simulations were performed with the real experimental parameters of the NSTX discharge under study (a$\approx$3650ρ_e) and with the real electron mass. Profiles of electron temperature and density at the relevant time during the discharge are imported from the TRANSP experimental database to initialize the simulations. The MHD numerical magnetic equilibrium is also read into the code and used for constructing the GTS field-line-following grid. We restrict our simulation domain to a radial section between r/a=0.21 and 0.32, which includes the scattering volume of the high-k experimental measurement. However, the full toroidal and poloidal angular extents are used. To resolve the ETG turbulence, a grid resolution of the order of the electron gyroradius is required in our simulation, imposing very stringent conditions. About 400 million grid points were used along with 23 billion particles.

Thanks to strong equilibrium $\mathbf{E}\times\mathbf{B}$ flows which may largely suppress ion temperature gradient modes (ITG) and trapped electron modes (TEM) in NSTX, couplings between ETG and low-k turbulence are limited. This allows us to assume adiabatic ions in our ETG simulations. The neoclassical equilibrium electric field, as calculated by the GTC-NEO code [11], is included in one of the simulations to assess its influence on the level of transport.

Fig. 1 shows the q profile, magnetic shear, and electron temperature in the simulated region of the NSTX discharge under study (shot #124901 at 300ms), which was a low density Helium plasma heated by the high harmonic fast wave (HHFW) RF technique. The measurements of coherent tangential scattering of electromagnetic waves for this discharge showed strong high-k activity, suggesting the presence of ETG turbulence [3]. A weak reversed shear exists in this region according to the profiles.

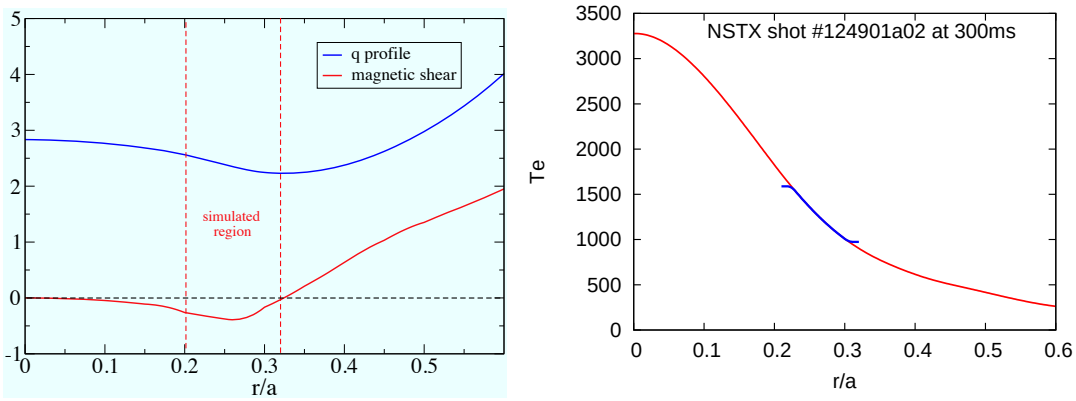

Figure 1: *Radial profiles of safety factor q, magnetic shear, and electron temperature in the simulated region of NSTX shot 124901.*

Since our simulations are fully self-consistent and do not include explicit sources and sinks, the ETG-driven transport causes significant relaxation in the electron temperature profile during the simulations as shown in the left panel of Fig. 2. This causes the effective drive $(\nabla T_{e0}+\langle\delta T_e\rangle_{\delta f})$ to decrease, which in turns makes the electron heat flux q_e drop with time. In order to quantify this effect and to model the sources of energy and particles that are present in the experiment, an anti-relaxation model was implemented in GTS to maintain a constant gradient drive during the simulation. We first assume a relaxed Maxwellian background distribution:

$$f_0(T_0+\langle\delta T\rangle)=f_0(T_0)+\delta f_0$$

$$\delta f_0 \approx (\frac{mv^2}{2T_0} - \frac{3}{2})\frac{\langle \delta T \rangle}{T_0} f_0, \text{ with } \delta T \equiv (1/3n)\int d\mathbf{v} m v^2 \delta f$$

We then remove the relaxation from the gradient drive:

$$\frac{D\delta f}{Dt} = -\{\mathbf{v}_E \cdot \nabla f_0 - \mathbf{v}_E \cdot \nabla \delta f_0 + \cdots\}$$

Validation simulations were carried out to test the anti-relaxation algorithm and it was found to be very successful. The right panel of Fig. 2 shows a GTS simulation of ITG turbulence for a DIIID tokamak discharge (shot #129533). In steady state, the constant gradient drive scheme raises the transport level to match the experimental value.

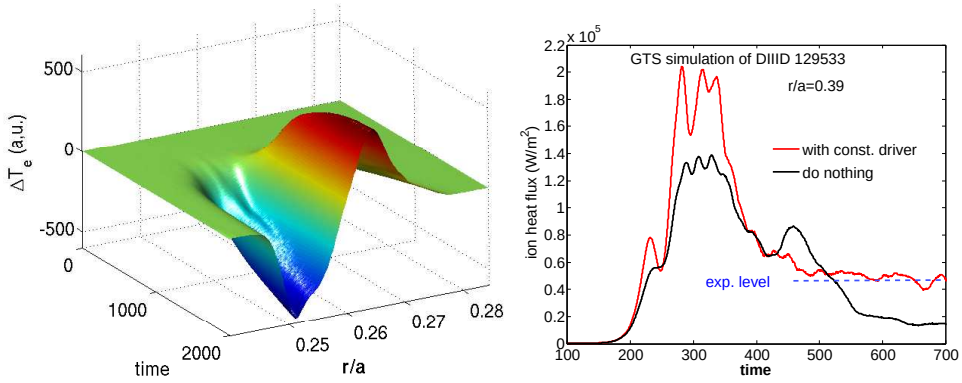

Figure 2: *Self-consistent relaxation of the electron temperature profile due to turbulence (left). Validation simulation of the constant drive algorithm in GTS (right). Maintaining a constant drive results in a transport level that matches the experimental value for the simulated DIIID case.*

3. Results

Our nonlinear ETG simulations of NSTX discharge 124901 show that in spite of the reversed shear observed in the experimental profiles, ETG turbulence readily develops in the simulated region as shown in Fig. 3 where isosurfaces of the electrostatic potential are displayed in a cut-tube cross section of the torus. Interestingly, the turbulence grows in two distinct regions although the one on the outside grows faster than the one on the inside (closer to the magnetic axis), indicating a stronger drive at that location.

Fig. 4 shows the temporal evolution of the flux surface averaged electron heat conductivity (χ_e) in the center of the outer region where the ETG turbulence is the strongest. The blue and black curves in the plot show the remarkable effect of self-consistent relaxation of the electron temperature profile due to the effect of ETG-driven transport on simulated turbulence and transport levels. The χ_e continues to decrease long after saturation in both cases. The red curve in the plot represents a simulation that includes the anti-relaxation scheme described in the previous section, which maintains a constant temperature gradient drive. Eliminating the influence of the profile relaxation is shown to be crucial in achieving a stationary turbulence steady state, and in determining the value of the electron heat flux. Taking into account the experimental uncertainties on the profiles, magnetic reconstruction, and overall plasma parameters, we carried out two simulations with a 20% increase in the temperature gradient (black and red curves in Fig. 4). Maintaining a constant drive at 20% higher than its value as calculated by TRANSP allows the simulation to reach a steady state at the level of the experimental value of χ_e. Given

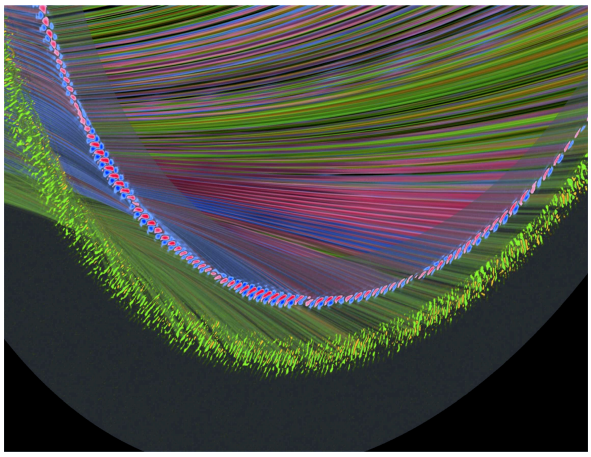

Figure 3: *Electrostatic potential structures generated by ETG turbulence. Two distinct regions of turbulence have developed by the time the outer region is in the saturated non-linear stage (image curtesy of K.-L. Ma, UC Davis, UltraVIS SciDAC Institute).*

that plasma profiles and parameters are subject to significant experimental errors, sensitivity studies of simulated ETG-driven electron thermal transport with respect to the local profiles of electron temperature, safety factor and effective charge number $Z_{\rm eff}$ need to be carried out. As shown in Fig. 4, both the ETG growth rate and saturated flux are increased by a factor of two as the electron temperature gradient is increased by 20%. Taking these effects into account, we conclude that, within experimental uncertainties in plasma profiles, the ETG turbulence can drive experimentally relevant transport for electron heat in NSTX.

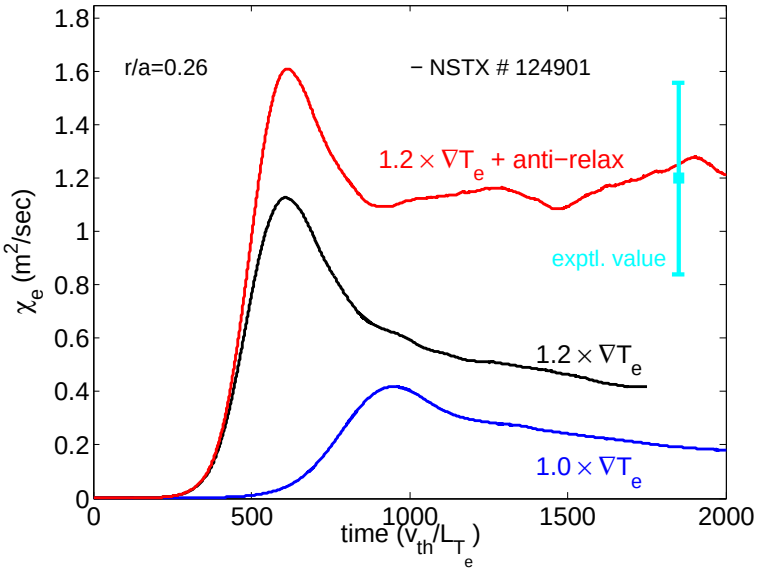

Figure 4: *Time histories of χ_e from global ETG simulations of an NSTX discharge and comparison with experimental estimate. The ∇T_e is boosted by 20% for red and black curves, and an "anti-relax" technique is used to maintain a constant ∇T_e drive for red curve.*

Our nonlinear ETG simulations also reveal remarkable new features with regard to nonlinear spectral dynamics in 2D perpendicular wavenumber space. Specifically, there exists direct, strong energy coupling between high-k ETG modes and electron geodesic acoustic modes (e-GAMs with high frequency and poloidal mode number $m = 1$), as illustrated in Fig. 5 where snapshots of the turbulence spectrum are presented (shown as k_r vs. k_θ 2D spectra) at 3 different times during the simulation. The first one ($t = 800\ \mathrm{v}_{th}/L_{Te}$) shows the linear stage during which the ETG linear modes are well defined and growing. However, an asymmetry is developing towards the lower k_θ values. The second snapshot shows the state of turbulence right after saturation ($t = 1200\ \mathrm{v}_{th}/L_{Te}$) and the cascading of the energy towards the longer wavelengths is evident. Additionally, a discrete mode, identified as the e-GAM, is clearly growing near $k_\theta = 0$. The last snapshot, which is well into the steady state of the simulation ($t = 2000\ \mathrm{v}_{th}/L_{Te}$), shows how the peak of the spectral energy has now moved away from the linear modes to the lower values of k_θ and even k_r. At the same time, zonal flows with fine radial scale are generated and continuously grow as shown in Fig. 6. This direct energy coupling may represent a new insight into the underlying mechanism for nonlinear ETG saturation. It also implies that the collisional damping of zonal flows and e-GAMs may have considerable impact on the formation of the steady state spectrum and saturation level. Moreover, the ETG fluctuations are characterized by strong anisotropy in the perpendicular wave number space with $k_r \ll k_\theta$ (Fig. 5), corresponding to radially elongated streamers emerging even in the well developed turbulence regime. The simulation predicted $k_\perp$ spectrum of density fluctuations is in general agreement with the experimental measurement using coherent scattering of electromagnetic waves [3] in the range of $k_\perp \rho_s \sim 5 - 15$, which is the range that the high-k scattering diagnostic covers.

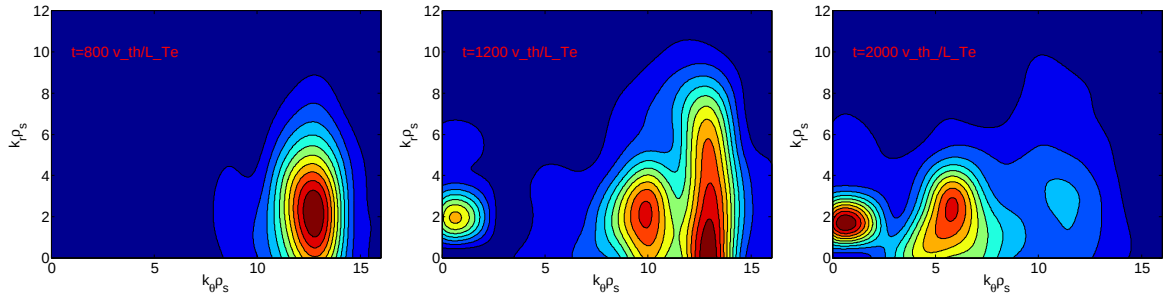

Figure 5: *Time evolution of 2D spectra of density fluctuations for the ETG simulation of NSTX described in this work.*

The experimental measurement of coherent tangential scattering looks at the density fluctuation spectra for 3 or 4 channels representing a particular wave number $k_\perp$, which is a combination of k_θ and k_r. At the steady state during our simulation we calculated the k_θ and k_r spectra of the density fluctuations and evaluated the exponential power of each one. Fig. 7 shows those spectra (left and center) as well as the experimental values (right panel). The exponential power is found to be between -2.6 (in k_r spectrum) and -5.3 (in k_θ) in the simulation compared to -4.5 of $k_\perp$ spectrum in experiments, which is consistent. However, ray-tracing calculations suggests the need for a more comprehensive synthetic diagnostic that takes into account the beam trajectories and experimental uncertainties. We are actively developing such a diagnostic and will apply it to our simulation data [12].

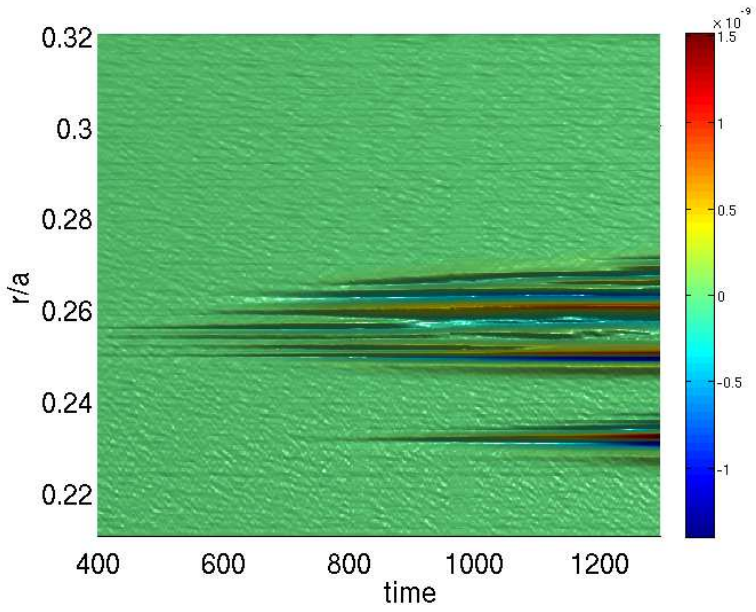

Figure 6: *Time evolution of the zonal flow.*

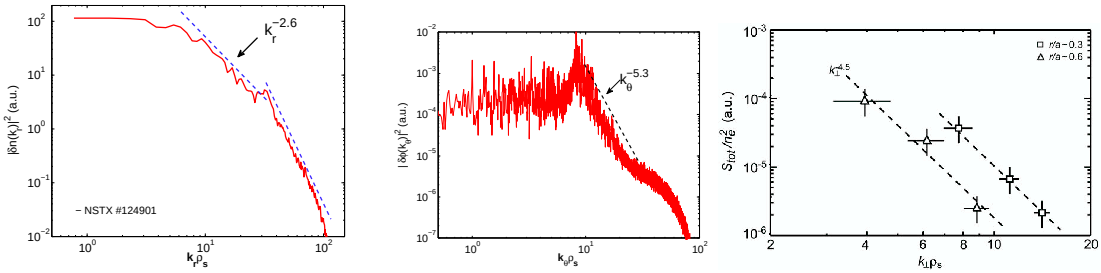

Figure 7: *Comparison of density fluctuation spectra from simulation and experiment (right panel, from Ref. [3]).*

4. Summary

Our global, nonlinear ETG simulations of NSTX indicate that ETG turbulence can drive experimentally relevant electron heat transport in NSTX. Indeed, maintaining the gradient drive constant while increasing its value by 20% brings the calculated χ_e to the experimental level. A more direct comparison with the actual experimental measurement of the density fluctuation spectra also reveals reasonably good agreement. However, a more detail synthetic diagnostic is needed for better comparison and is currently under development.

References

[1] D. R. Smith *et al.*, Rev. Sci. Instr. **79**, 123501 (2008).

[2] D. R. Smith *et al.*, Phys. Plasmas **16**, 112507 (2009).

[3] E. Mazzucato *et al.*, Nucl. Fusion **49**, 055001 (2009).

[4] S.M. Kaye *et al.*, Phys. Rev. Lett. **98**, 175002 (2007).

[5] W. X. Wang *et al.,* Phys. Plasmas **13**, 092505 (2006).

[6] A. M. Dimits *et al.,* Nucl. Fusion **47**, 817 (2007).

[7] J. Candy *et al.,* Plasma Phys. Contr. Fusion **49**, 1209 (2007).

[8] W. Dorland *et al.,* Phys. Rev. Lett. **45**, 5579 (2000).

[9] Z. Lin *et al.,* Phys. Plasmas **12**, 056125 (2005).

[10] A. Bottino *et al.,* Phys. Plasmas **14**, 010701 (2007).

[11] W. X. Wang *et al.,* Comp. Phys. Comm. **164**, 178 (2004).

[12] F. Poli *et al.,* Phys. Plasmas *in press*.

Acknowledgements

This work was supported by U.S. DOE Contract No. DE-AC02-09CH11466 and the SciDAC project for Gyrokinetic Particle Simulation of Turbulent Transport in Burning Plasmas. This research used resources of the National Center for Computational Sciences at Oak Ridge National Laboratory, which is supported by the Office of Science of the U.S. Department of Energy under Contract No. DE-AC05-00OR22725.